

Separately contacted edge states at high imbalance in the integer and fractional quantum Hall effect regime

E.V. Deviatov^{1,*} and A. Lorke²

¹*Institute of Solid State Physics RAS, Chernogolovka, Moscow District 142432, Russia*

²*Laboratorium für Festkörperphysik, Universität Duisburg-Essen, Lotharstr. 1, D-47048 Duisburg, Germany*

(Dated: March 18, 2008)

This review presents experimental results on the inter-edge-state transport in the quantum Hall effect, mostly obtained in the regime of high imbalance. The application of a special geometry makes it possible to perform $I - V$ spectroscopy between individual edge channels in both the integer and the fractional regime. This makes it possible to study in detail a number of physical effects such as the creation of topological defects in the integer quantum Hall effect and neutral collective modes excitation in fractional regime. The while many of the experimental findings are well explained within established theories of the quantum Hall effects, a number of observations give new insight into the local structure at the sample edge, which can serve as a starting point for further theoretical studies.

PACS numbers: 73.43.-f, 73.33.Fj, 73.43.Jn, 72.25.Dc, 72.20.Ht

I. INTRODUCTION: EDGE STATES AT LOW IMBALANCE

Both the integer quantum Hall effect (IQHE) and the fractional quantum Hall effect (FQHE) occur in high-mobility two-dimensional electron systems in a quantizing magnetic field under low temperatures. Although the Fermi level is within the spectrum gap in both regimes, the origins of the gap are substantially different for the IQHE and FQHE. The integer quantum Hall effect is explained by the Landau quantization in the spectrum of the two-dimensional electron system in a magnetic field. On the contrary, the FQHE is fully recognized as a manifestation of the electron-electron interaction. Despite these differences, charge transport is mostly determined by edge effects in both IQHE and FQHE regimes. The present report is dedicated to a detailed investigation of intra-edge transport and the differences and similarities in the physical effects observed in both regimes.

A. Edge states definition

Halperin¹ introduced current-carrying edge states as the intersections of the Landau levels and the Fermi level near the sample edges. Hence, the total number of edge states is equal to the filling factor, i.e., the number of filled Landau levels, and their electrochemical potentials are equal to the electrochemical potentials of the corresponding edges of the sample. If the number of filled Landau levels is n , the total current through the sample can be written as $I = n(e/h)\Delta\mu$, where $\Delta\mu$ is the difference in the electrochemical potentials of the sample edges. Hence, the current is determined only by the difference in electrochemical potentials of the edges (or, in other words, of the edge states) and the number of filled Landau levels (the number of edge states). If we introduce the edge-state current $(e/h)\mu$, then the sum of all edge-state currents gives the total current through the

sample.

Büttiker² combined Halperin's idea of current-carrying edge states with the Landauer formalism³, aiming to take scattering in one-dimensional semiconductors into account. He showed that the effects of elastic and nonelastic scattering in edge states and contacts can be taken into account by introducing the transmission coefficient matrix T_{ij} . He suggested the formalism for calculating various resistances for samples with many ohmic contacts. In this formalism, the current I_i carried by edge states going from a contact i is given by

$$I_i = \frac{e}{h} \left(n_i \mu_i + \sum_{j \neq i} T_{ij} \mu_j \right), \quad (1)$$

where I_i is the current through edge states, going from the contact i , μ_i is the electrochemical potential of the contact i , n_i is the number of edge states that are going from the contact i . It is worth to mention here, that edge-state transport is dissipativeless in the absence of inter-edge scattering. A finite resistance is arising due to the mixing of the electrochemical potentials in ohmic contacts.

B. Experiments at low imbalance

Experimental verification of Büttiker's formalism was performed mainly in the Hall-bar geometry with crossing gates (see Fig. 1). In this geometry, a sample with two current leads (1 and 4 in Fig. 1) and several potential contacts (2 and 3 in Fig. 1) was crossed by one or several gates. Reducing the electron concentration under the gates to the smaller than the bulk filling factor results in a nonzero voltage between potential contacts in the quantum Hall effect regime. The result can easily be explained in terms of edge states: in the absence of gate voltage, two edge states leave contact 2 and the same

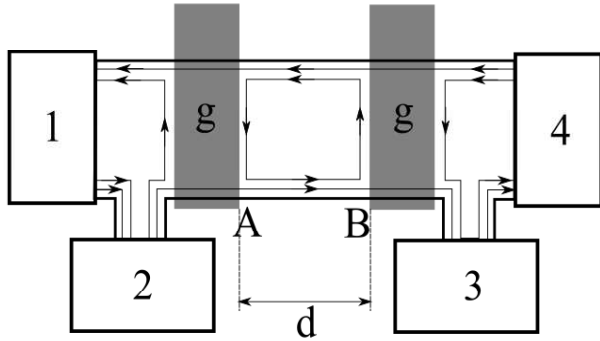


FIG. 1: Hall-bar geometry with two crossing gates. Numbered rectangles denote ohmic contacts. Shaded areas are gates evaporated onto the sample. The structure of edge states is shown for the filling factors $g = 1$ under the gate and $b = 2$ in the rest of the sample. (After Ref. 5)

states arrive at contact 3, see Fig. 1. Because no current flows through the potential contacts, their electrochemical potentials are equal, leading to zero voltage drop between contacts. If the filling factor beneath the gates is reduced, then some of the edge states are reflected at the gate boundary while the others pass through, which leads to a more complicated set of electrochemical potentials of the contacts. It can be calculated from Büttiker formulas (1) for the particular situation. Moreover, this geometry allows to model and study various effects considered by Büttiker. A very comprehensive review of experiments in this geometry is made in Ref⁴.

In the region between the gates in Fig. 1, one of the edge states starts from beneath the gate and the other approaches the gate along the gate edge. Their electrochemical potentials are different in general. Further along the sample edge, the electrochemical potentials of these states come to an equilibrium due to the electron transport between them, i.e., across the sample edge. Thus, the transport effects between the edge states can be studied if the mixing of states in the contact can be excluded, i.e., if a second crossing gate is used as a detector of the final electrochemical potential of the edge state, as shown in Fig. 1. Using the Büttiker formalism (1), it is easy to see that the measured resistance is

$$R_{14,23} = \frac{h}{e^2} \left[1 + \exp \left(-\frac{2d}{l_{eq}} \right) \right]^{-1}, \quad (2)$$

where l_{eq} is the phenomenological equilibration length between the edge states. It can therefore be found from the deviation in the measured resistance from the quantized value.

Experimental data obtained by various groups (see, e.g., Ref.⁵) have shown that the equilibration length between spin-split edge states can reach 1 mm at low temperatures and is of the order of 100 μm for ones separated by a cyclotron splitting. This difference is caused by the fact that the spin flip accompanying the electron trans-

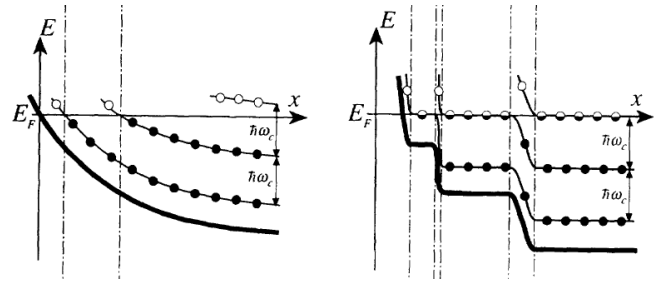


FIG. 2: Edge structure for the smooth edge potential (After Ref 9). Left panel: simple one-particle picture. Right panel: edge reconstruction because interaction effects.

fer is hampered at the edge of the sample: there are no magnetic impurities in perfect heterostructures, and the spin flip is due to the spin-orbital and hyperfine interactions^{5,6,7,8}.

We note that such experiments provide information about the equilibration processes only for a small imbalance (a small difference in electrochemical potentials in comparison to the spectral gaps) between the edge states. In fact, any initial imbalance can be applied, but to have measurable deviations from the quantized value in (2), $l_{eq} \sim d$ should be fulfilled. Thus, the resulting processes are at low imbalances, between the edge states that are practically in equilibrium. The physical origin is the following: in the Hall-bar geometry we study transport across the edge as the some correction to the constant transport along the edge. At high imbalances this correction is too small to be investigated. Thus, Hall-bar geometry is very suitable to study undisturbed situation at the sample edge. At high imbalances, however, edge reconstruction can be anticipated, following a lot of interesting physical effects. For the investigations in this regime we should switch to the Corbino topology.

C. Edge structure in real samples

Before describing the special features of the transport between the edge states in the case of an arbitrary imbalance, where the details of the edge structure manifest themselves, we give a detailed description of the structure of a real (in most cases, etched or electrostatic) edge of a sample.

The edge potential is *smooth* if it varies on a length scale much larger than the magnetic length. This is true for usual experimental realizations in the integer quantum Hall effect regime, e.g. etched mesa edge or the electrostatic confinement, because of high values of the spectral gaps and the long-range character of the Coulomb potential. In the case of a smooth potential, the bottom of the two-dimensional subband rising up in approaching the edge of the sample, and the Landau levels follow the subband bottom (Fig. 2). At any point, a local filling factor (the number of filled levels) can be

introduced, which varies from its initial value in the bulk of the sample to zero at the edge. A change in the local filling factor occurs each time a Landau level crosses the Fermi level, see Fig. 2, left. Chklovsky et. al.⁹ took the electron-electron interaction into account in the mean-field approximation. It turned out that one-dimensional intersections of the Fermi and Landau levels are transformed into finite-width strips (in a certain region, the Landau level is ‘pinned’ to the Fermi level, see Fig. 2, right) where the local filling factor gradually varies, and the edge of the electron system is an alternating sequence of compressible and incompressible strips of electronic liquid. The incompressible strip width is determined by the energy gap between the corresponding Landau levels. The strips of compressible and incompressible electron liquid can be observed directly in spatially resolved techniques, see, e.g., Ref.¹⁰.

In this case, we should answer the question about the current distribution over the sample. It was clearly showed by Thouless¹¹ that dissipationless (diamagnetic) currents flow in regions with a potential gradient because the group velocity in such areas is nonzero. It means that they are concentrated in the incompressible strips at each sample edge. If the electrochemical potentials of the edges are different, the current in one direction exceeds the opposite current by exactly the value determined by the difference in the electrochemical potentials of the edges. This justifies the validity of the Büttiker formalism, which is sensitive only to integral characteristics, such as the electrochemical potentials of the edges and the matrix of scattering coefficients ‘from contact to contact.’ This consideration pertains to the current along the edge of the sample. The current running across the edge and equilibration of the edge states is determined by tunnelling through incompressible strips and diffusion in compressible ones.

Taking these considerations into account, we can reformulate the definition of an edge state as a *compressible* strip. This provides a clear definition for the electrochemical potential of an edge state and keeps our consideration consistent with the above considerations, where an edge state was defined as the intersection of a Landau level with the Fermi level.

II. TRANSPORT BETWEEN EDGE STATES AT HIGH IMBALANCE IN THE INTEGER QUANTUM HALL EFFECT REGIME

Most probably, a quasi-Corbino geometry in combination with the technique of a crossing gate was first proposed in Ref.¹². But the first experimental results appeared only ten years later¹³, when a measurement method appropriate for obtaining interpretable results was developed and the experimental difficulties arising in such measurements were overcome. By that time, the idea of applying the Corbino geometry had been thoroughly forgotten, and the authors of Ref.¹³ had to de-

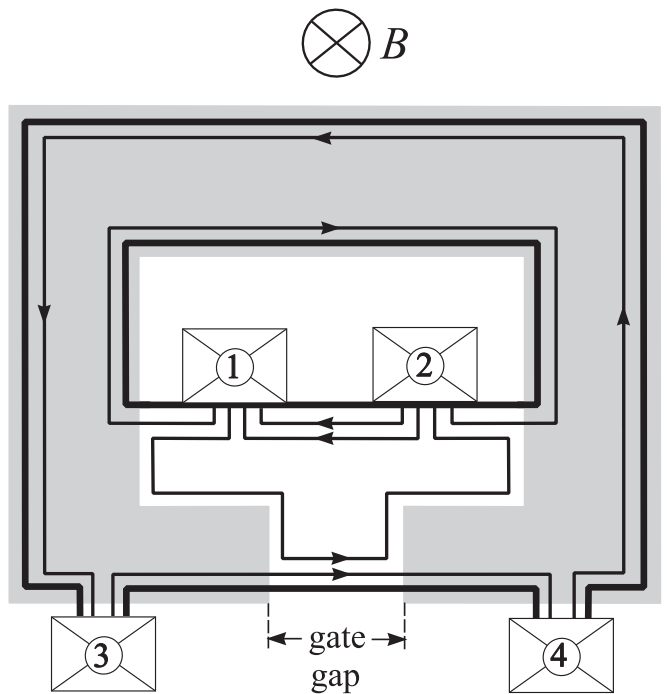


FIG. 3: Sketch of a sample in the quasi-Corbino geometry (After Ref. 18). Bold lines show the inner and outer edges of the mesa, crossed rectangles with numbers denote ohmic contacts, the shaded area is the gate. The structure of the edge states is shown in the case where the filling factor is $g = 1$ under the gate and $\nu = 2$ outside the gate.

velop the sample geometry anew.

A. Quasi-Corbino experimental geometry

In the quasi-Corbino geometry (see Fig. 3), the sample has the rectangular shape with an etched region at the center, which creates two independent edges not connected topologically. Ohmic contacts are made to the two-dimensional electron gas (2DEG) at both edges. A metal gate is evaporated on the top of the sample. It surrounds the internal etched area, leaving only a T-shaped region of the two-dimensional gas between the outer and inner boundaries uncovered (see Fig. 3).

By partially depleting the 2DEG under the gate, different filling factors in the T-shaped region (ν) and under the gate (g) can be achieved, $g < \nu$. Some part of the edge states are reflected at the boundary of the gate and go along the gate to the other boundary of the sample. At the inner boundary of the sample not covered by the gate (the ‘bar’ of the T), all edge channels are in equilibrium due to the macroscopic size and several ohmic contacts. At the outer boundary of the sample, the area not covered by the gate (the ‘leg’ of the T), is of several micrometers in size. It is much less than the equilibration length at low temperatures, and there are no ohmic contacts here. Thus, if a voltage is applied to a pair of

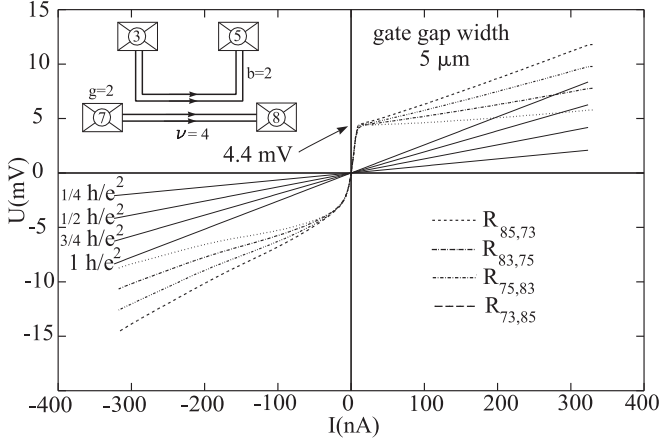


FIG. 4: Current-voltage characteristics at a high temperature (straight lines, 4K, complete equilibration) and a low temperature (non-linear curves, 30 mK, non-equilibrium regime) for the transport between cyclotron-split edge states (After Ref. 13).

contacts at the inner and outer edges, a difference in electrochemical potentials appears between the edge states at the outer edge of the sample, in the area not covered by the gate, i.e. in the gate-gap region.

To obtain $I - V$ characteristics of the transport between edge states in the gate-gap, 4-point configuration is used. A dc current is applied between a pair of inner and outer contacts and the resulting dc voltage is measured between another pair of inner and outer contacts. (Due to the existence of a preferred direction determined by the magnetic field, there are four principally different combinations of contacts.) Four-point configuration allows to eliminate contact effects. The obtained results were qualitatively confirmed by direct measurements of two-terminal $I - V$ characteristics.

This geometry offers many degrees of freedom to a researcher. By varying the filling factor in the gate-gap area with the help of a magnetic field, the total number of interacting edge channels can be changed; by varying the filling factor beneath the gate with the help of the gate voltage, the channels can be divided into groups to which the difference in electrochemical potentials is applied and between which the current flows. In particular, the transport between edge states separated by a spin or cyclotron gap or, in double-layer structures, by symmetric-antisymmetric (isospin) splitting can be studied in the IQHE regime.

B. Switching from the low imbalance to the high imbalance case

Transformation of the $I - V$ curves was demonstrated with decreasing the temperature¹³. At a high temperature (4 K), the $I - V$ s are linear, with the slope exactly corresponding to its equilibrium value obtained

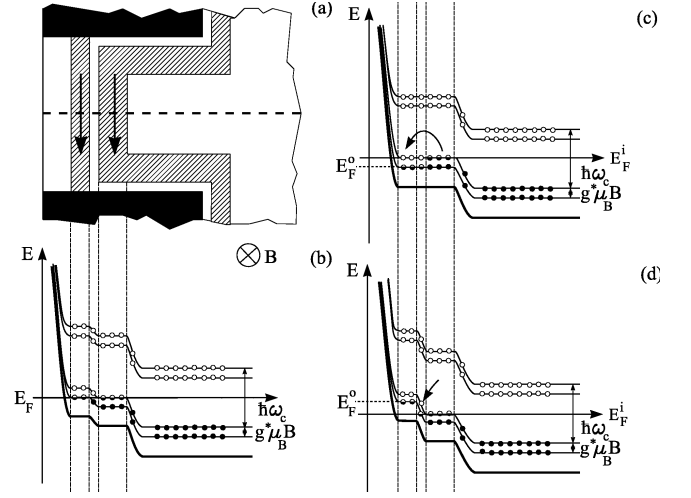


FIG. 5: (Left panel) The structure of the sample edge in the interaction area of edge states in equilibrium. The bulk filling factor ν is equal to 2. Two spin-split energy levels reach the edge and form a structure of compressible and incompressible strips. (Right panel) The structure of the sample edge in the interaction area of edge states in the case of a voltage applied between compressible strips. At positive voltage, because the electron charge is negative, the potential barrier between the edge states reduces down to the flat-band situation (c). At negative voltage, the barrier grows and deforms (d). (After Ref. 13).

from the Büttiker calculation (1) for various combinations of ohmic contacts (see Fig. 4). This fact can be explained by the small value of the equilibration length (compared to the size of the interaction area length, i.e. gate-gap width) at this temperature. As the temperature decreases to 30 mK, the equilibration length grows dramatically⁵, and the system enters the regime of strong imbalance. The current-voltage characteristic becomes strongly nonlinear and asymmetric (see Fig. 4), with a pronounced threshold behavior of the right-hand branch (corresponding to positive currents when the inner contact is grounded). Above the threshold, this branch is linear, while the left-hand branch has no threshold and remains nonlinear. A similar transformation of the $I - V$ was observed at low temperatures¹⁴ as a result of *in situ* varying the length of the interaction area.

C. Interpretation of the non-linear current-voltage characteristics

The above mentioned non-linear $I - V$ curves can only be explained¹³ by means of the smooth edge model, in which the edge is represented by alternating strips of compressible and incompressible electron liquids (see Fig. 2 and Fig. 5, which -for simplicity- discusses the case $\nu = 2$). At bulk filling factor $\nu = 2$, the interaction area near the outer boundary contains two compressible strips separated by the incompressible strip with the lo-

cal filling factor $g = 1$. The electrochemical potential of each compressible strip is determined by the electrochemical potential of the corresponding (inner or outer) ohmic contact. If a voltage is applied to a pair of contacts situated at different edges, a difference in electrochemical potentials drops within the incompressible strip between the two compressible ones and affects the distribution of edge potential in it. For instance, at positive voltages (inner contacts grounded), the potential barrier between the edge states decreases and completely disappears when the voltage is equal to the corresponding spectral gap (see Fig. 5 (c)). This leads to a dramatic growth in the current at this voltage and to a complete equilibration between the edge states at larger potential differences. At negative bias voltage, the potential barrier increases, which leads to the appearance of a strongly nonlinear $I - V$ branch.

D. Spectral investigations

Thus, the energy gap between the edge states can be found from the position of the threshold voltage on the right-hand (positive) $I - V$ branch. It turns out that the gap is equal to the bulk value of splitting between the corresponding energy levels. This fact was first demonstrated for cyclotron gaps¹³, which justifies using the smooth-edge model and experimentally confirms the smoothness of an etched edge in the IQHE regime. (All the arguments for the $I - V$ should also be valid in the case of a sharp edge, but the measured gap is then much larger than the bulk value of the splitting). For sufficiently pure samples, it was shown in¹⁵ that the gap between spin-split edge states corresponds to the bulk exchange-increased Lande factor¹⁶.

E. Equilibration at the edge

In addition to spectroscopic studies, the process of equilibration was studied in Ref.¹⁷, with the initial values of imbalance exceeding the spectral gap in the transport between cyclotron-split edge states. In this experiment, the slope of the linear (above- threshold) part of the $I - V$ right-hand branch was studied (see Fig. 4). It turned out that for strongly nonequilibrium edge states, not the whole difference of electrochemical potentials but only the part exceeding the spectral gap can be redistributed.

Furthermore, the Büttiker formalism² was modified by explicitly introducing a local characteristic of the transport between the edge states instead of the integral matrix T_{ij} . Namely, the local transport parameter α was defined as the ratio of the distributed difference in electrochemical potentials between the edge states and the difference in electrochemical potentials allowed for redistribution. This single parameter α is universal: it fully describes the slopes of linear parts of the $I - V$ for any combination of the contacts and depends only on the

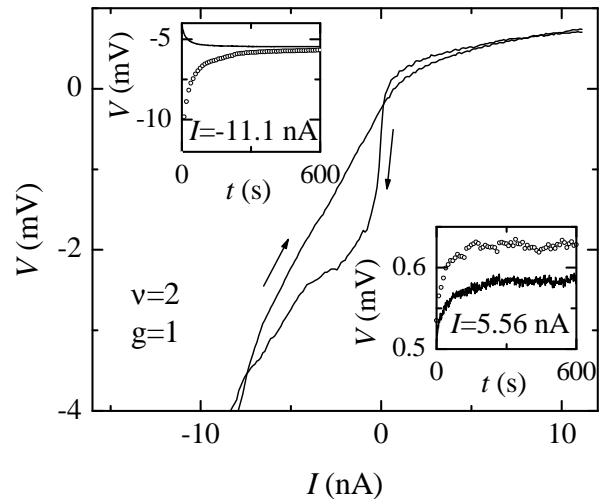


FIG. 6: Hysteresis for the $I - V$ for the spin- flip transport and relaxation curves (After Ref. 18).

physics of the transport between edge states. Numerical values of α indicate the extent to which equilibrium is established between the edge states.

F. Spin-flip transport: creation of dynamic nuclear polarization

The transport between spin-split edge states should be accompanied by the electron spin flip. The spin flip is mainly provided by the spin-orbital interaction⁵, but part of the electrons participate in the so-called flip-flop process: due to the hyperfine interaction, the spins of the electron and the nucleus are flipped simultaneously. This process, even at relatively high temperatures, leads to the creation of an area with a dynamic polarization of nuclear spins, in which the static polarization by the external magnetic field is inessential^{7,8}.

Creation of dynamic nuclear polarization has been studied in the strongly nonequilibrium case in Ref.¹⁸, where the $I - V$ s were measured for the transport between spin-split edge states in the quasi-Corbino geometry. Under these conditions, the current-voltage characteristics exhibit a considerable hysteresis, especially pronounced in the left- hand (negative) branch (see Fig. 6). Comparison with the $I - V$ obtained for transport without the spin flip (through a cyclotron gap) in the same field and with the same degree of disorder showed that the hysteresis is not related to the spurious transient effects such as recharging of the sample from the contacts. It was shown in Ref.¹⁸ that the hysteresis is caused just by the dynamic polarization of the nuclei in the interaction area of the sample. Indeed, the effective Overhauser field arising in this case influences the spin splitting, which determines the potential barrier between the edge states. This affects on the current for all electrons, and not only

for those whose spin flipping is caused by the flip-flop process; as a result, a noticeable hysteresis of the $I - V$ occurs.

In addition, relaxation processes investigated in Ref.¹⁸ revealed two typical relaxation times, of the order of 25 and 200 s (see the insets in Fig. 6). The first time corresponds to the creation of the dynamic nuclear polarization area at a certain stage of the transport between the edge states, and the second relates to the development of a stable area where nuclear spins in the sample are polarized due to the competition between the nuclear spin diffusion and the escape of the spins from the system.

It was also demonstrated¹⁹ that the flip-flop mechanism can be reversed. After establishing a local dynamic nuclear polarization region, the externally applied current is switched off, and the sample exhibits an output voltage, which decays with a time constant typical for the nuclear spin relaxation.

G. Edge states in the double quantum wells. Topological defects in the edge state structure

More complicated for investigation are tunnel-coupled double electron layers, or double-layer systems, which are usually realized in double quantum wells separated by a tunnel-transparent barrier. Because of the tunnelling between the layers, the bulk spectra of such systems are already rather complicated^{20,21,22,23,24,25}. At the edge of the sample, the Fermi level becomes the same for edge states that originate, in the general, from different parts of the quantum well or from subbands, depending on the quantum well symmetry.

In the symmetric case, in addition to the cyclotron and spin splitting, a symmetric-antisymmetric splitting appears, which is smaller than the Zeeman splitting in strong fields and exceeds it in weak fields^{23,24,25}. In intermediate fields, where these splitting values should be comparable, a new phase, the so-called antiferromagnetic one, appears due to the electron-electron interaction²⁶. A bulk transition into this phase from the range of weak fields was observed in Ref.²⁵ and from the range of strong fields in Ref.²⁴. Thus, singularities can be expected in the transport between edge states in the vicinity of the bulk phase transition point. Such transport singularities were observed in Ref.²⁷, where the incompressible strip separating edge states was demonstrated to disappear near the bulk phase transition point.

An important fact, established in Ref.²⁷, is that the structure of edge states always corresponds to the structure of the bulk spectrum and follows even its complicated transformations. It was investigated by mapping the energy gaps at the edge using $I - V$ spectroscopy, while the system approach the phase transition point.

The Pauli principle does not forbid the intersection of edge states corresponding to different quantum numbers (see, for example, Fig. 7). Such intersections were called defects in the topological structure of edge states,

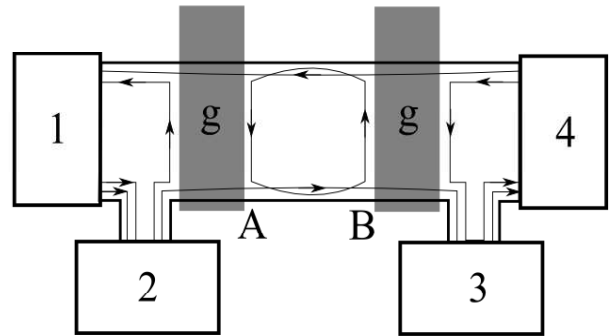


FIG. 7: The simplest example of the topological defects in the edge states structure (After Ref. 29).

or topological defects. The possibility of the existence of such defects was shown theoretically in Refs^{28,29}.

The only way to detect topological defects is by studying the transport between edge states, which can be most conveniently done in the quasi-Corbino geometry¹³. The existence of a gate in this geometry, in particular, allows changing the symmetry of the quantum well, and hence the energy spectrum under the gate^{21,22}. Since the structure of edge states corresponds to the structure of the bulk spectrum²⁷, the quasi-Corbino geometry allows to realize topological defects in the structure of edge states³⁰: (i) If the well is asymmetric in the interaction area of the edge states, then edge-state electrons are fully described by the spin and isospin (layer number) orientations²¹. Electrons injected from beneath the gate can also come either from an isospin-polarized state or from a mixed one. In the latter case, because the injection occurs with isospin conservation, the electrons are distributed among the edge states. This results in the intersections of edge states and in the equilibration of electrochemical potentials for all edge states in the interaction area, which manifests itself in the perfect linearity of the $I - V$ in a normal magnetic field. (ii) If a tangential field is applied, the states in the interaction area become isospin-mixed²², and the topological defects disappear. This leads to a strongly nonlinear $I - V$, usual for the inter-edge-state transport. In this way, the existence of topological defects and the possibility of controlling their creation and disappearance were demonstrated in Ref.³⁰.

III. TRANSPORT BETWEEN EDGE STATES AT HIGH IMBALANCE IN THE FRACTIONAL QUANTUM HALL EFFECT REGIME

A. Laughlin's wavefunction and the composite fermion hypothesis. Edge states in the FQHE

In the fractional quantum Hall effect regime, the system has to be treated as a large number of strongly interacting particles, and therefore no method exists for ex-

actly solving the problem with the real Hamiltonian. The interaction results in a rearrangement of the ground state of the system of particles, and the new ground state cannot be obtained from the perturbation theory as a small correction to the interaction-free state. Two approaches turned out to be efficient for the description of such a liquid: the method of a trial ground-state wave function (the Laughlin approach³¹) and the mean-field method³² (based on the hypothesis of composite fermions).

According to MacDonald³³ there are collective gapless excitation modes at the sample edge in the FQHE regime, that he defined as edge states. The structure of the excitation spectrum was shown to correspond to the structure of the Laughlin's ground state at the particular filling factor. For example, the state with $\nu = 2/3$, according to Laughlin, is constructed as a quasi-hole state on the background of a completely filled lowest Landau level. Correspondingly, in this case, edge spectrum consists from the branches, originating from quasi-holes and electrons correspondingly. He attributed a current to each excitation branch $I = (e^*/h)\Delta\mu$, where $e^* = e\nu$ is the effective charge of the branch ($1/3$ and -1 in the above example) and completed the construction of a FQHE Büttiker formalism² by introducing the transmission matrix T_{ij} .³³

The so-defined edge excitations are one-dimensional and in the FQHE regime the inter-electron interaction must be consistently taken into account. This was done in the theoretical works by Wen³⁴, who applied the Luttinger model³⁵ of a one-dimensional interacting liquid to this problem and demonstrated that collective excitations with a gapless spectrum do exist at the edge and their structure is indeed determined by the hierarchical structure of the bulk ground state. Physically, these excitation branches correspond to different modes of edge magnetoplasmons (see, e.g.,³⁶ that we will need below). We note that an edge state in the FQHE regime is probably the only exact realization of a chiral Luttinger liquid model: the edge creates the one-dimensionality of the system, the bulk states form an infinite reservoir, which is necessary in the Luttinger model, and the magnetic field determines a preferred direction providing the chirality of the electron liquid. Therefore, the investigation of collective excitations in the FQHE regime allows studying a rare example of a non-Fermi electron liquid.

Since the transport along the edge is determined by the bulk filling factor and edge electrochemical potentials³³, the only way to study Luttinger liquid effects is the transport across the edge. Wen³⁴ has shown theoretically that the tunnel density of states has power-law behavior in the FQHE regime, $D(E) \sim E^{1/g-1}$ with $g = 1/\nu$ for the filling factors ν from the principal Laughlin sequence. It was also shown in³⁷ that there are universal scaling relations for the temperature dependence of the tunnel density of states $D \sim T^{1/g}$. These results have also been confirmed in the approach of composite fermions³⁸.

In the experimental study of tunnelling into the edge, it must be ensured that the $I - V$ nonlinearity is caused precisely by the excitation of collective modes and not by

the deformation of the edge potential. For this, the so-called cleaved edge overgrowth technique³⁹ is used. Experiments in Refs^{39,40} demonstrated power-law $I - V$ s in the case of tunnelling into the edge, as well as temperature scaling of these diagrams with the exponents close to the predicted ones^{34,37} for the filling factor $\nu = 1/3$. The experiment and the theory give considerably different results⁴⁰ outside the vicinity of $\nu = 1/3$, which might be caused by a structure of compressible and incompressible strips forming at the edge³⁹.

Numerical calculations based on the Laughlin wave function⁴¹ and in the framework of the composite-fermion approach⁴² showed that the structure of strips of an incompressible and compressible electron liquid already appears at the edge width as small as five or six magnetic lengths. In other words, all real potentials (such as, for instance, the most common potential of a mesa etched edge) satisfy this condition. The situation is still not so clear for the cleaved edge overgrowth (CEO) samples^{39,40}, which are the best candidates for the sharp edge realization. On the one hand, there are signs of the compressible-incompressible strips formation in high magnetic fields³⁹, supporting the above mentioned calculations^{41,42}. On the other hand, there are signs of the sharp edge situation⁴³ in low magnetic fields, at much higher magnetic length. This difference could also occur from the progress in the CEO samples preparation over a decade. In this Review we will concern only the high-field limit, as the most appropriate for the FQHE regime.

For a smooth potential, the bottom of the two-dimensional subband increases in the vicinity of the edge and the electron concentration decreases. Hence, a local filling factor can be introduced, which varies from the bulk value to zero in approaching the edge of the sample. Beenakker⁴⁴ showed that for a sufficiently pure system and the FQHE existing with such local filling factors, finite-width incompressible strips corresponding to these filling factors appear on the edge. In the FQHE regime, therefore, similarly to the IQHE case, a smooth edge consists of alternating strips of compressible and incompressible electron liquid. The difference from the integer case lies in the fact that it is now impossible to introduce a system of Landau levels bent at the edge, because everything occurs on the last (single) Landau level. It can only be asserted that there is no gap in the compressible strips, while a gap corresponding to the electrochemical potential between the ground and the excited states occurs in the incompressible strips. This gap shrinks at the edges of each incompressible strip. Dissipation-free current, similarly to the IQHE case, is carried by the ground state and, because the 'excess' current is concentrated near the edge of the incompressible area in the absence of equilibrium, it can be described as an edge current.

As in the integer case, the analogue of the Büttiker

formalism can now be introduced as⁴⁴:

$$I_i = \frac{e}{h} \left(\nu_i \mu_i + \sum_{j \neq i} T_{ij} \mu_j \right), \quad (3)$$

where I_i is the current carried by the edge states coming out of contact i , μ_i is the electrochemical potential of contact i , and ν_i is the maximum filling factor for incompressible strips coming from contact i . It is easy to see that equation 3 contains Büttiker formula 1 as a special case of integer ν_i , as well as MacDonald's result³³ for a sharp edge potential, because $e^* = e\nu$. This indicates that Büttiker formalism is a rather general integral relation, which is independent of the details of the edge structure. Similarly to the integer case, to check the formalism one should place a crossing gate on the sample. Such experiments showed a perfect agreement between the calculation and the measurement⁴⁵.

While strips of incompressible electron liquid exist at a smooth edge of a two-dimensional electron system in the FQHE regime, collective modes appear near the boundaries of these strips⁴¹. In addition, because the edges of the strips are close (both to each other and to the edges of neighboring strips if the potential is not very smooth), and the electric fields are long-range ones, these modes interact⁴⁶. Therefore, collective excitations on a smooth edge in the FQHE are most similar to neutral magnetoplasmon modes, which were first proposed for the IQHE regime³⁶. As a result, in the case of tunnelling into a smooth FQHE edge, the exponent of the tunnel density of states and hence the $I-V$ s become dependent on the real shape of the edge potential⁴⁶, although the $I-V$ maintains its power-law behavior, which was demonstrated in Ref.⁴⁰.

B. Transport across the incompressible strip at high imbalance

As it was shown before, there are two major problems in investigation of collective effects at the smooth sample edge in FQHE regime: (i) a presence of the structure of compressible and incompressible strips, which entangle different collective modes at the strip edges; (ii) deformation of the edge potential by the applied voltage V while measuring $I-V$ curves. This affects the $T_0(V)$ dependence, where T_0 is one-particle barrier transmittance, and, therefore, makes it difficult to separate one-particle effects and the collective ones. The former problem can be removed by separate contacting to compressible strips across a single incompressible one. The latter problem demands the high-imbalance regime. Indeed, collective effects can be selected in two limiting cases. The first is where the bias potential is so small compared to the potential barrier that it does not deform it (This regime was realized in Ref.⁴⁰, but without separate contacting to the strips). The second case is where the bias potential is large in comparison with the barrier width. The

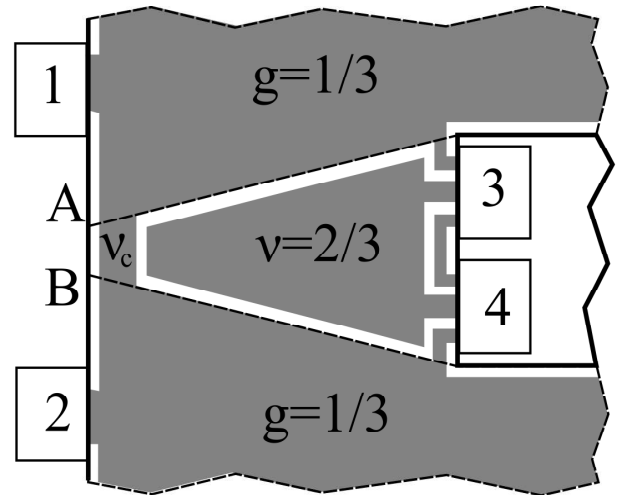


FIG. 8: Schematic diagram of the active region of the sample in the quasi-Corbino geometry. The etched mesa edges are shown by solid lines, the dashed lines represent the split-gate edges. The gate-gap region at the outer mesa edge is denoted as AB. Light gray areas are the incompressible regions at filling factors ν (in the bulk), g under the gate ($g < \nu$), and at local filling factor ν_c ($\nu_c = g$) in the incompressible stripe at the mesa edges. Compressible regions (white) are at the electrochemical potentials of the corresponding ohmic contacts, denoted by bars with numbers. (After Ref. 47)

barrier is deformed and other deformation has no effect on transport across it. (This fact can be easily understood in a triangular barrier approximation). We note that the second case is easier to realize from the experimental standpoint, and it can be better controlled. Thus, experiments in the quasi-Corbino geometry are needed to study collective effects at the smooth sample edge.

Figure 8 shows the structure of compressible and incompressible electron liquid strips near the gate gap of the sample in the quasi-Corbino geometry for the simple situation of filling factors $g = 1/3$ under the gate and $\nu = 2/3$ outside it. This scheme is based on the data of magnetoresistance and magnetocapacitance measurements. For instance, measuring the magnetoresistance in the quantum Hall effect regime allows finding the field corresponding to the filling factor $\nu = 2/3$ in the part of the sample not covered by the gate. Further, the capacitance between the two-dimensional system and the gate should be measured while decreasing the electron concentration under the gate. This allows finding the FQHE fractional filling factors manifested in the given sample at given magnetic fields due to a decrease in the electron concentration. Because approaching the edge is also accompanied by a decrease in the electron concentration for the smooth edge potential, we can be sure that incompressible strips appear at the edge of the sample at the same filling factors that were observed when decreasing the electron density beneath the gate. For example,

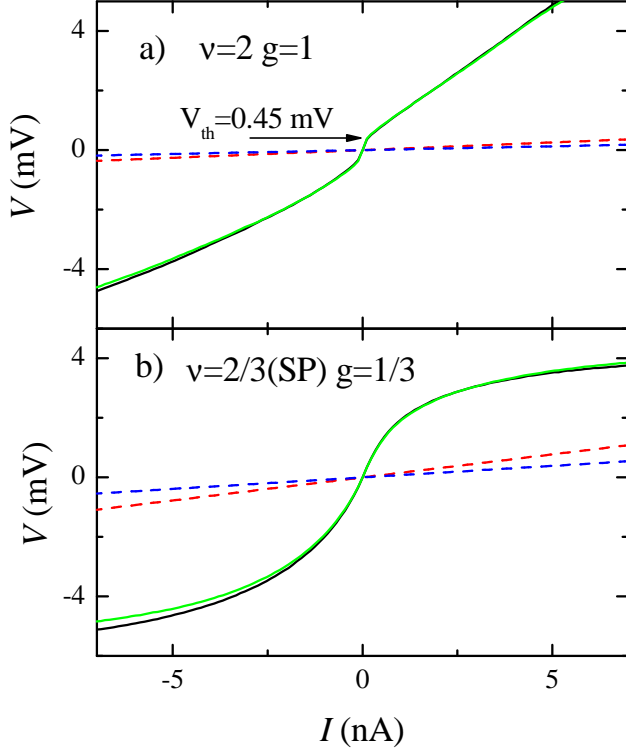


FIG. 9: $I - V$ curves for integer filling factors $\nu = 2, g = 1$ (a) and fractional ones $\nu = 2/3, g = 1/3$ (b) for two different contact configurations for a sample with an extremely narrow gate-gap width $L_{AB} = 0.5 \mu\text{m}$. Equilibrium lines (with $R_{eq} = 2; 1h/e^2$ (top) and $6; 3h/e^2$ (bottom)) are shown. Magnetic field B equals to 1.67 T for integer fillings and to 5.18 T for fractional ones. (After Ref. 47).

in the sample described in Ref.¹⁵, at the bulk filling factor $\nu = 1$, incompressible strips appear in the vicinity of the edge at local filling factors $2/3$ and $1/3$. Choosing the filling factor under the gate to coincide with one of these values, we choose the incompressible strip for which the transport is studied.

Similarly to the IQHE case, obtaining current-voltage characteristics is the basic tool in the study of the transport. Measurement of the transport through an incompressible strip can be carried out in two ways: by fixing the current or by fixing the voltage. Because the FQHE is especially sensitive to the quality of the samples and the ohmic contacts, to check the results for reliability it is necessary to see whether the data of both above-described methods of the $I - V$ measurement agree in each particular case. In addition, it is necessary to independently estimate the resistance and the quality of the ohmic contacts using magnetoresistance measurements, to use various samples and different methods to cool them, and to compare the results with the ones known for the IQHE regime.

We consider a current carried across an incompressible strip, shown in Fig. 8, depending on the equilibration

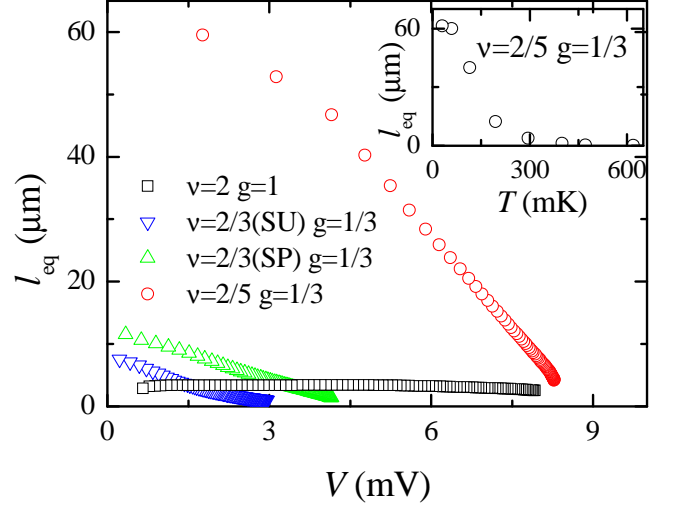


FIG. 10: Equilibration length l_{eq} for different filling factor combinations as function of the voltage imbalance V across the incompressible stripe with corresponding local filling factor $\nu_c = g$ (see caption to Fig. 8). Inset shows an example of the temperature dependence of the l_{eq} for $\nu = 2/5, g = 1/3$ ($B = 7.69$ T). (After Ref. 47).

length l_{eq} :

$$I = R_{eq}^{-1} V (1 - \exp(-L_{AB}/l_{eq})), \quad (4)$$

For the gate-gap width $L_{AB} \ll l_{eq}$, the shape of the current-voltage characteristic directly reflects the behavior of the equilibration length as the imbalance between the edge states is varied. In turn, the equilibration length reflects the behavior of the transition probability w between the edge states, $l_{eq} \sim w^{-1}$. The transition probability w can be written as the single-particle transmittance T_0 of the potential barrier times the tunnel density of states D : $w \sim T_0(V)D(V, T)$. As mentioned before, the barrier can be considered triangular in the strongly nonequilibrium case, and therefore the single-particle transmittance, which can be written as $\exp(-C\Delta^{3/2}/V)$, tends to unity when the imbalance exceeds the fractional gap $\Delta \ll V$. Because the equilibration length for fractional filling factors and small imbalances are known^{8,48,49} to be of the order of $10 \mu\text{m}$, the samples used in Ref.⁴⁷ had the width of their working area $L_{AB} = 0.5 \mu\text{m}$.

Figure 9 shows examples of $I - V$ s for integer and fractional filling factors in samples with small interaction area. The differences in the $I - V$ s for fractional filling factors from the well-known $I - V$ s for integer filling factors (see above) are (i) the absence of a threshold; (ii) strong nonlinearity within the whole voltage range; and (iii) almost perfect symmetry. This behavior of the $I - V$ s is observed for almost all fractional filling factors.

Equilibration lengths calculated by means of equation 4 for various filling factors are shown in Fig. 10. For integer filling factors, the l_{eq} behavior corresponds to the

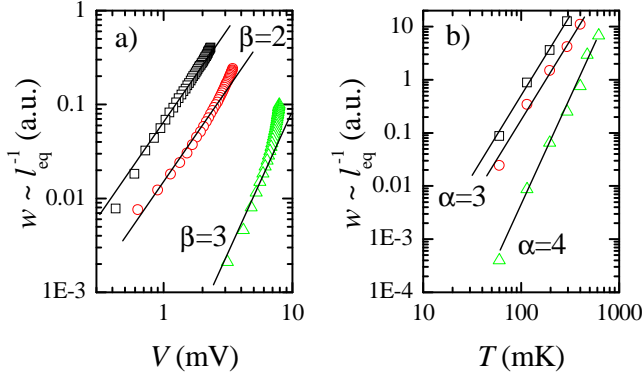


FIG. 11: Transition probability $w \sim l_{eq}^{-1}$ is shown as a function of the temperature (a) and of the voltage imbalance at $T = 30$ mK (b) in logarithmic scales, demonstrating the power-law dependencies. The filling factors are $\nu = 2/3(SU)$, $g = 1/3$ (squares); $\nu = 2/3(SP)$, $g = 1/3$ (circles); $\nu = 2/5$, $g = 1/3$ (triangles). (After Ref. 47).

one discussed in section II, known one caused by the deformation of the potential barrier between edge states, while for fractional filling factors, the behavior of l_{eq} was studied in Ref.⁴⁷ for the first time.

Under the conditions of the experiment⁴⁷, the dependence of the transition probability $w \sim l_{eq}^{-1}$ (see Fig. 11) on bias and temperature reflects the dependence of the tunnel density of states D on these parameters. The power-law behavior of the transition probability was demonstrated in Ref.⁴⁷ (see Fig. 11); the exponents found in experiment for the voltage and temperature dependencies differ by unity, as indeed should be the case under the excitation of collective modes^{34,37}. Thus, neutral excitations⁴¹ do exist at the edges of the incompressible strip and determine transport across it at high imbalances in the FQHE regime.

The exponents were found in Ref.⁴⁷ for the first time and need a theoretical explanation. They are different for the filling factors $\nu = 2/3, g = 1/3$ and $\nu = 2/5, g = 1/3$ which is caused by the collective-mode excitation at the boundary of the bulk filling factor $\nu = 2/5$. The edge of the $\nu = 2/5$ bulk incompressible state is extremely close to the incompressible strip with local filling factor $\nu_c = 1/3$ in this case, because of $\nu - \nu_c \ll \nu$. Thus, we can expect some influence in D also from the edge excitations of $\nu = 2/5$ bulk incompressible state, affecting the exponents in power-law $D(V, T)$. Thus, the structure of the collective excitations is more complicated at $\nu = 2/5$, resembling the acoustic modes predicted in Ref.³⁶.

C. Equilibration at the edge and the structure of the excitation spectrum

Direct measurements of the structure of edge collective excitations (in the cases where the structure is assumed to be complicated, see Ref³³) are not realistic: they would

require an independent study of several simultaneously propagating magnetoplasmon modes^{36,41}. But an indirect measurement method is possible. During the equilibration from an initially strongly nonequilibrium case, the transport across the incompressible strip involves excitation of collective modes⁴⁷, which, in turn, establish the edge potential and therefore influence the equilibration⁵⁰. Such effects are not taken into account by the single-particle Büttiker-Beenakker theory^{2,44}. Hence, the comparison between the experimental equilibrium resistance and the one calculated according to Büttiker's formalism (1,3), can indicate a structure of the collective excitations.

In Ref.¹⁵ equilibration was studied through incompressible strips corresponding to the local filling factors $\nu_c = 2/3$ and $1/3$, at the bulk filling factor $\nu = 1$. This allows investigating equilibration at the same strip structure in the gate-gap by realizing contacts between different compressible strips. Büttiker's formulas (1,3) yields the same equilibrium values of resistance for both combinations of filling factors. However, the experiment¹⁵ showed the equilibrium resistance values to be different: for the transport through the incompressible strip with the local filling factor $\nu_c = 2/3$, the slope of the equilibrium curve turned out to be much smaller than the expected one, while for the transport through the strip with the filling factor $\nu_c = 1/3$, the measured slope was close to the expected one. In terms of Büttiker's formalism, *smaller* equilibrium slope corresponds to an excess charge transfer across the incompressible strip, which is difficult to explain in the framework of one-particle picture. At the same time, the filling factor $2/3$ is distinguished in this experiment only by the fact that for the edges of the strip $3/2$, a complicated structure of collective modes is expected^{33,34,41}, and interaction between these modes determines the 'excess' equilibration of edge states. Thus, the experiment¹⁵ for the first time demonstrated the existence of several branches of collective excitations at the edge of an FQHE system with the filling factor $2/3$.

In Ref.¹⁴, the influence of collective modes on the equilibration at the edge was studied under the variation of the gate gap width. The study was aimed at transforming a strongly nonlinear current-voltage characteristic into a linear one without changing the state of the two-dimensional electron system in the sample. For this, the structure of the sample in the quasi-Corbino geometry was modified: the gate-gap area was made macroscopically large. In this area, an additional gate was placed. Varying the voltage at the additional gate allows controlling the width of the interaction area between 10 and 800 μm .

Transformation of current-voltage characteristics for the filling factors $\nu = 2/3, g = 1/3$ is shown in Fig. 12. As expected, the $I - V$ curves, initially weakly nonlinear, turn into linear ones with the slope coinciding with the one found from the Büttiker-Beenakker calculation (1,3). The linearity of the central part of the curves

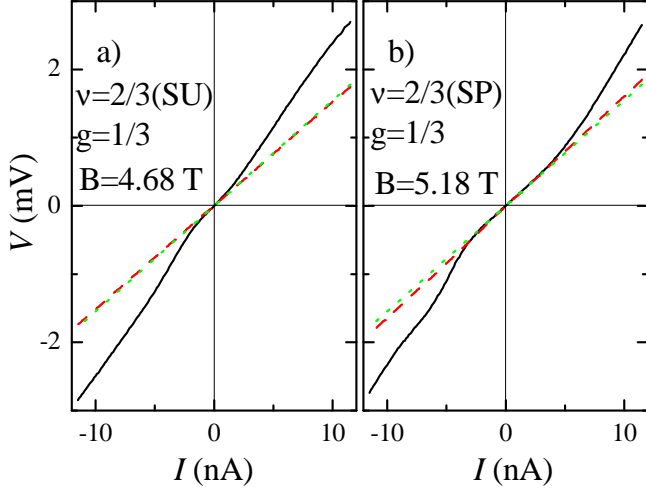


FIG. 12: $I-V$ curves for fractional filling factors $\nu = 2/3$, $g = 1/3$ for narrow ($10 \mu\text{m}$, solid line) and wide ($800 \mu\text{m}$, dashed line) interaction regions, for two spin configurations of $\nu = 2/3$: (a) spin unpolarized (SU) state ($B = 4.68 \text{ T}$); (b) spin polarized (SP) state ($B = 5.18 \text{ T}$). Equilibrium curve (with $R_{eq} = 6h/e^2$) is shown by dots. (After Ref. 14).

means that the equilibration length does not exceed the interaction area size at small imbalances. Based on these considerations, the equilibration length can be estimated to be $10 \mu\text{m}$, which is in agreement with the results in Refs^{8,48,49} obtained at small imbalances.

The most unexpected result is the transformation of $I-V$ s corresponding to the filling factors $\nu = 2/5$, $g = 1/3$ (see Fig. 13). From the weakly nonlinear $I-V$, which is situated above the the calculated equilibrium line, the equilibration length for edge states can be estimated to exceed $10 \mu\text{m}$. As the interaction area increases, the $I-V$ still remains weakly nonlinear (see the inset in Fig. 13) but lies below the equilibrium calculated curve, which would correspond, in terms of the Beenakker-Büttiker single-particle picture, to *excessive* charge transfer (by more than a quarter). Nonlinear curves for both lengths of the interaction area can be reduced to a single curve by scaling along the current axis. In this case, the scaling coefficient $q = 2.35$ is 40 times less than the ratio of the interaction area lengths.

We note that prior to Ref.¹⁴, no edge-state experiments have been carried out for filling factors other than $2/3$ and $1/3$. It was predicted⁵⁰ however, that collective modes at the "non-third" edge are expected to have a considerable impact on the equilibration process. As it was mentioned above, in Ref.¹⁴ at filling factors $\nu = 2/5$, $g = 1/3$ the edge of the $2/5$ bulk state has an influence on the transport effects, because of the small width of the corresponding compressible strip. Thus, the result¹⁴ is not too unexpected and can be interpreted as the influence of the collective effects on the equilibration process.

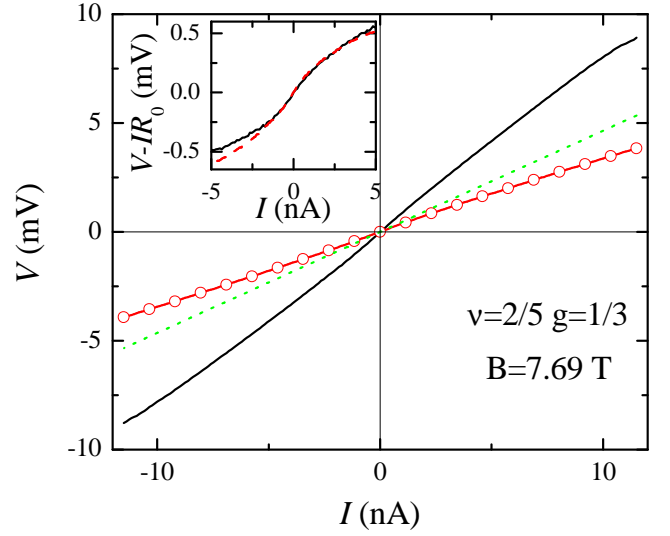


FIG. 13: $I-V$ curves for fractional filling factors $\nu = 2/5$, $g = 1/3$ for narrow ($10 \mu\text{m}$, solid line) and wide ($800 \mu\text{m}$, line with open circles) interaction regions. Equilibrium curve (with $R_{eq} = 18h/e^2$) is shown by dots. Inset shows the wide-region curve (dash), scaled to the narrow-region one (solid) in current direction. The linear dependence IR_0 with $R_0 = 28h/e^2$ is subtracted to highlight the non-linear behavior. Magnetic field B equals to 7.69 T . (After Ref. 14)

IV. CONCLUSION

We summarize the main results of the edge-state investigations in the IQHE and FQHE regimes:

- The edge potential of a real system can be considered smooth in both the IQHE and FQHE regimes. At the edge, there is a structure of compressible and incompressible strips of electron liquid.
- The Büttiker formalism is sensitive only to integral values, such as the electrochemical potentials of the edges and total scattering between the edge states. Therefore, it is not sensitive to the edge structure and many-body effects. Thus, it is valid for low imbalances in both the IQHE and FQHE regimes
- The structure of edge states for double-layer tunnel-coupled systems corresponds to the structure of the bulk spectrum and even follows its considerable rearrangements in the IQHE regime. This leads to a possibility of topological defects appearing in the edge state structure.
- Equilibration among the edge states occurs by means of the electron transport through incompressible strips. This process is fully governed by the single-particle tunnel transparency of the barrier in such strips in IQHE regime. In contrast, in the FQHE regime the tunnel density of states has an impact on all effects related to the transport between edge states, both in the direct studies of

the transport and in the studies of equilibration between edge states. This many-body tunnel density of states is governed by the so-called neutral collective excitations at the edge.

Acknowledgments

We wish to thank V.T. Dolgoplov for fruitful discussions. We gratefully acknowledge financial support by

the RFBR, RAS, the Programme "The State Support of Leading Scientific Schools", Deutsche Forschungsgemeinschaft, and SPP "Quantum Hall Systems", under grant LO 705/1-2. E.V.D. is also supported by MK-4232.2006.2 and Russian Science Support Foundation.

-
- * Corresponding author. E-mail: dev@issp.ac.ru
- ¹ B. I. Halperin, Phys. Rev. B **25**, 2185 (1982).
 - ² M. Büttiker, Phys. Rev. B **38**, 9375 (1988).
 - ³ R. Landauer, Phil. Mag. **21**, 863 (1970)
 - ⁴ R.J. Haug, Semicond. Sci. Technol. **8**, 131 (1993).
 - ⁵ G. Müller, D. Weiss, A. V. Khaetskii, K. von Klitzing, S. Koch, H. Nickel, W. Schlapp, and R. Lösch, Phys. Rev. B **45**, 3932 (1992).
 - ⁶ A. V. Khaetskii, Phys. Rev. B **45**, 13777 (1992).
 - ⁷ David C. Dixon, Keith R. Wald, Paul L. McEuen and M. R. Melloch, Phys. Rev. B **56**, 4743 (1997).
 - ⁸ T. Machida, S. Ishizuka, T. Yamazaki, S. Komiyama, K. Muraki and Y. Hirayama, Phys. Rev. B **65**, 233304 (2002).
 - ⁹ D. B. Chklovskii, B. I. Shklovskii, and L. I. Glazman, Phys. Rev. B **46**, 4026 (1992).
 - ¹⁰ E. Ahlswede, J. Weis, K. v. Klitzing, K. Eberl, Physica E, **12**, 165 (2002).
 - ¹¹ D.J. Thouless, Phys. Rev. Lett. **71**, 1879 (1993).
 - ¹² G. Müller, E. Diessel, D. Weiss, K. von Klitzing K. Ploog, H. Nickel, W. Schlapp, and R. Lösch, Surf. Sci. **263**, 280 (1992)
 - ¹³ A. Würtz, R. Wildfeuer, A. Lorke, E. V. Deviatov, and V. T. Dolgoplov, Phys. Rev. B **65**, 075303 (2002).
 - ¹⁴ E.V. Deviatov *et. al.*, Phys. Rev. B **74**, 073303 (2006).
 - ¹⁵ E. V. Deviatov, V. T. Dolgoplov, A. Lorke, W. Wegscheider, A.D. Wieck, JETP Lett., **82**, 539 (2005).
 - ¹⁶ V.T. Dolgoplov *et. al.*, Phys. Rev. Lett. **79**, 729 (1997).
 - ¹⁷ E. V. Deviatov, V. T. Dolgoplov, A. Würtz, JETP Lett. **79**, 618 (2004).
 - ¹⁸ E. V. Deviatov, A. Würtz, A. Lorke, M. Yu. Melnikov, V. T. Dolgoplov, D. Reuter, A. D. Wieck, Phys. Rev. B **69**, 115330 (2004).
 - ¹⁹ A. Würtz, T. Muller, A. Lorke, D. Reuter, and A. D. Wieck, Phys. Rev. Lett. **95**, 056802 (2005)
 - ²⁰ A.G. Davies, C.H.W. Barnes, K.R. Zolles, J.T. Nicholls, M.Y. Simmons, and D.A. Ritchie, Phys. Rev. B **54**, R17331 (1996).
 - ²¹ V. T. Dolgoplov, A. A. Shashkin, E. V. Deviatov, F. Hastreiter, M. Hartung, A. Wixforth, K. L. Campman, and A. C. Gossard Phys. Rev. B **59**, 13235 (1999).
 - ²² Deviatov E.V., Khrapai V.S., Shashkin A.A., V. T. Dolgoplov, F. Hastreiter, A. Wixforth, K. L. Campman, A. C. Gossard, JETP Lett **71**, 496 (2000).
 - ²³ A. Sawada, Z. F. Ezawa, H. Ohno, Y. Horikoshi, A. Urayama, Y. Ohno, S. Kishimoto, F. Matsukura, and N. Kumada Phys. Rev. B **59**, 14888 (1999).
 - ²⁴ V. Pellegrini, A. Pinczuk, B.S. Dennis, A.S. Plaut, L.N. Pfeiffer, and K.W. West, Phys. Rev. Lett. **78**, 310 (1997); Science **281**, 799 (1998).
 - ²⁵ V. S. Khrapai, E. V. Deviatov, A. A. Shashkin, V. T. Dolgoplov, F. Hastreiter, A. Wixforth, K. L. Campman, and A. C. Gossard, Phys. Rev. Lett. **84**, 725 (2000).
 - ²⁶ S. Das Sarma, S. Sachdev, and L. Zheng, Phys. Rev. Lett. **79**, 917 (1997);
 - ²⁷ E. V. Deviatov, A. Würtz, A. Lorke, *et. al.*, JETP Lett., **79**, 171 (2004).
 - ²⁸ Jed Dempsey, B. Y. Gelfand, and B. I. Halperin Phys. Rev. Lett. **70**, 3639 (1993); B. Y. Gelfand and B. I. Halperin Phys. Rev. B **49**, 1862 (1994).
 - ²⁹ Lex Rijkels and Gerrit E. W. Bauer, Phys. Rev. B **50**, 8629 (1994).
 - ³⁰ E. V. Deviatov, V. T. Dolgoplov, A. Würtz, A. Lorke, A. Wixforth, W. Wegscheider, K. L. Campman, and A. C. Gossard, Phys. Rev. B **72**, 041305 (2005)
 - ³¹ R. B. Laughlin, Phys. Rev. Lett. **50**, 1395 (1983).
 - ³² J.K. Jain, Phys. Rev. Lett. **63**, 199 (1989).
 - ³³ A. H. MacDonald, Phys. Rev. Lett. **64**, 220 (1990).
 - ³⁴ Xiao-Gang Wen, Phys. Rev. B **43**, 11025 (1991); Phys. Rev. Lett. **64**, 2206 (1990); Phys. Rev. B **44**, 5708 (1991).
 - ³⁵ J.M. Luttinger, J. Math. Phys. **4**, 1154 (1963)
 - ³⁶ I.L. Aleiner and L.I. Glazman, Phys. Rev. Lett. **72**, 2935 (1994).
 - ³⁷ C.L. Kane and M.P.A. Fisher, Phys. Rev. B **46**, 15233 (1992); Phys. Rev. Lett. **68**, 1220 (1992).
 - ³⁸ A.V. Shytov, *et. al.*, Phys. Rev. Lett. **80**, 141 (1998).
 - ³⁹ A. M. Chang, L. N. Pfeiffer, and K. W. West, Phys. Rev. Lett. **77**, 2538 (1996).
 - ⁴⁰ M. Grayson, D. C. Tsui, L. N. Pfeiffer, K. W. West, and A. M. Chang, Phys. Rev. Lett. **80**, 1062 (1998); M. Hilke, D. C. Tsui, M. Grayson, L. N. Pfeiffer, and K. W. West, Phys. Rev. Lett. **87**, 186806 (2001).
 - ⁴¹ C. d. C. Chamon and X. G. Wen, Phys. Rev. B **49**, 8227 (1994).
 - ⁴² Dmitri B. Chklovskii, Phys. Rev. B **51**, 9895 (1995).
 - ⁴³ M. Huber, M.Grayson, M. Rother, W. Biberacher, W. Wegscheider, and G. Abstreiter, Phys. Rev. Lett. **94**, 016805 (2005).
 - ⁴⁴ C. W. J. Beenakker, Phys. Rev. Lett. **64**, 216 (1990).
 - ⁴⁵ D. A. Syphers and P. J. Stiles, Phys. Rev. B **32**, 6620 (1985); R. J. Haug, A. H. MacDonald, P. Streda and K. von Klitzing, Phys. Rev. Lett. **61**, 2797 (1988); S. Washburn, A. B. Fowler, H. Schmid and O. Kem, Phys. Rev. Lett. **61**, 2801 (1988); S. Komijama, H. Hira, S. Sasoand and S. Yiyamizu, Phys. Rev. B **40**, 5176 (1989).
 - ⁴⁶ S. Conti and G. Vignale, Phys. Rev. B **54**, 14309 (1996).
 - ⁴⁷ E. V. Deviatov *et. al.*, EPL, **77**, 37002 (2007).

- ⁴⁸ L. P. Kouwenhoven, B. J. van Wees, N. C. van der Vaart, C. J. Harmans, C. E. Timmering, and C. T. Foxon, Phys. Rev. Lett. **64**, 685 (1990).
- ⁴⁹ A. M. Chang and J. E. Cunningham, Phys. Rev. Lett. **69**, 2114 (1992).
- ⁵⁰ U. Zülicke and E. Shimshoni, Phys. Rev. B **69**, 085307 (2004); U. Zülicke and E. Shimshoni, Phys. Rev. Lett. **90**, 026802 (2003).